Supplementary Information

Tailoring Non-Fullerene Acceptors to Enhance Molecular Ordering in Inverted Bilayer Organic Solar Cells

Deyang Xie [1], Shilin Chen [1], Ming Wang [1], Lanlan Zhang [1], Xiaoge Huang [1], Sein Chung [2], Young Yong Kim [2], Kilwon Cho [2], Zhenmin Zhao [1, 3]*, Zhipeng Kan [1]

[1] Center on Nanoenergy Research, Institute of Science and Technology for Carbon Peak & Neutrality, School of Physical Science & Technology, Guangxi University, Nanning 530004, China.

[2] Department of Chemical Engineering, Pohang University of Science and Technology, Pohang 37673, South Korea.

[3] Institute of Materials Research, Tsinghua Shenzhen International Graduate School, Tsinghua University, Shenzhen, 518055 China.

* Corresponding author, E-mail: 2007401038@st.gxu.edu.cn.

Content

1. Materials

PM6, N3, Y6 and BTP-eC9 were purchased from Solarmer, Inc (Beijing). L8-BO was purchased from Dongguan Volt-Amp Optoelectronics Technology Co., Ltd. Polydimethylsiloxane (PDMS) was purchased from Hangzhou WISECREATE Technology Co., Ltd. All materials were used as received without further purification.

2. Preparation of the ZnO Nanoparticles

In a 500 ml beaker, dissolve 10 mmol of anhydrous zinc acetate in 125 ml of methanol and heat the mixture to 60°C while stirring. Gradually add 1.1 g of KOH dissolved in 50 ml of methanol. After reacting for 20 minutes, add 1 ml of ethanolamine. Concentrate the mixture to a volume of 20 ml, then add ethyl acetate to precipitate the product. Centrifuge and discard the supernatant. Dissolve the precipitate in 8 ml of ethanol, then add ethyl acetate to precipitate again and centrifuge. Combine the precipitate with anhydrous ethanol and dissolve it using ultrasonic treatment, achieving a concentration of approximately 30 mg/ml.

3. Methods

Inverted bilayer OSCs were fabricated in a conventional device configuration of ITO/ZnO/NFAs/PM6/MoO3/Ag. The glass substrates coated with a layer of indium tin oxide (ITO, 15 Ω/sq) (device area: 0.0361 cm^2). Substrates were prewashed with isopropanol to remove organic residues before immersing in an ultrasonic bath of soap for 15 min. Samples were rinsed in flowing deionized water for 5 min before being sonicated for 15 min each in successive baths of deionized water, acetone, and isopropanol. Next, the samples were dried with pressurized nitrogen before being exposed to an UV-ozone plasma for 15 min. After that, ZnO 4500 rpm. was spun coated on ITO, heated at 150℃ for 15 min, and then transferred to a glove box filled with N2 for later use. Among these, the PDMS with specifications of hardness 42 Shore A,

tensile strength 4.2 MPa, elongation at break 180%, and elastic modulus 0.6 MPa was selected. Cut the PDMS into pieces corresponding to the size of the glass slides. Attach the PDMS pieces to the glass slides and transfer them to a glove box. Soak the attached PDMS in isopropanol for 20 minutes. For OSCs with an inverted bilayer architecture, non-fullerene acceptors (NFAs, 14 mg/mL in chloroform) were stirred at 50 °C for 2 h. Subsequently, 15 μL of this solution was spin-coated onto ZnO substrates at 3500 rpm to form the first layer. PM6 (4 mg/mL in chloroform) was then spin-coated onto a pre-patterned PDMS stamp under identical conditions (15 μL, 3500 rpm) and transferred onto the NFA layer to fabricate the inverted bilayer active layer. Finally, 2nm thick MoO_3 and 100 nm thick Ag electrode was thermally deposited under vacuum conditions of 2×10^{-5} Pa.

The J-V measurement was performed via a XES-50S1 (SAN-EI Electric Co., Ltd.) solar simulator (AAA grade) whose intensity was calibrated by a certified standard silicon solar cell (SRC-2020, Enlitech) under the illumination of AM 1.5G 100 mW cm^{-2}. The AM 1.5G light source with a spectral mismatch factor of 1.01 was calibrated by the National Institute of Metrology. The intensity of the AM 1.5G spectra was calibrated by a certified standard silicon solar cell (SRC-2020, Enlitech) calibrated by the National Institute of Metrology. The J-V curves of small-area devices were measured in forwarding scan mode (from -0.2 V to 1.2 V) with a scan step length of 0.02 V. The external quantum efficiency (EQE) was measured by a certified incident photon to electron conversion (IPCE) equipment (QE-R) from Enli Technology Co., Lt. The light intensity at each wavelength was calibrated using a standard monocrystalline Si photovoltaic cell. Optoelectronic characterizations were performed with PAIOS (Fluxim, Switzerland).

4. UV-Vis Absorption

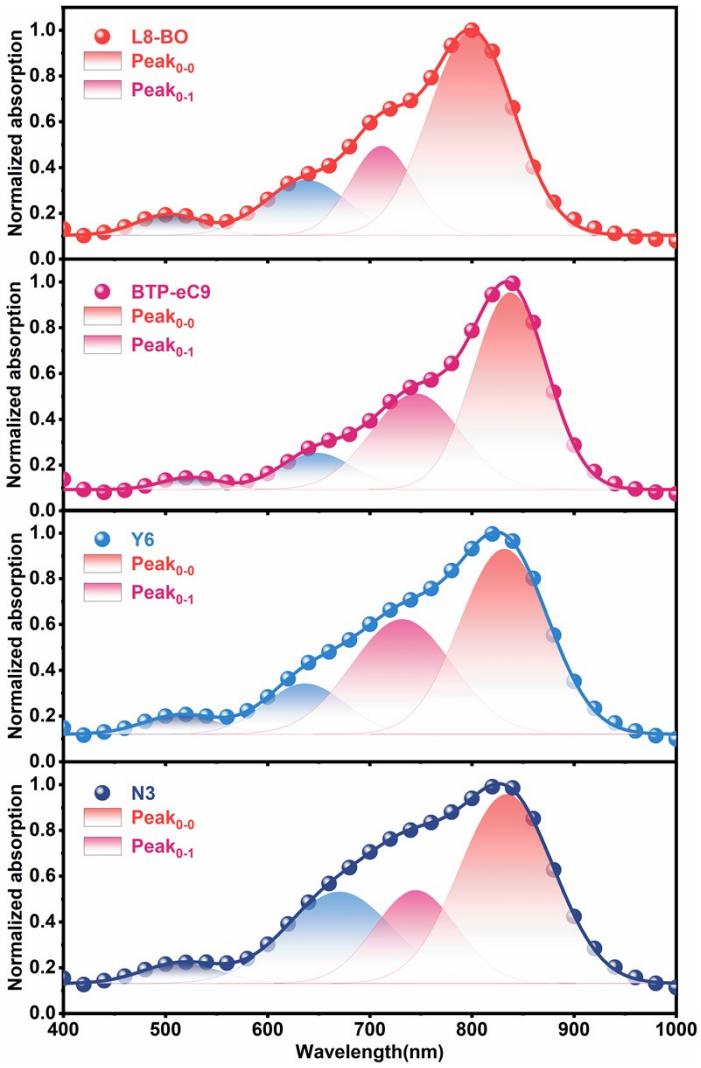

Figure S1. Normalized UV Vis absorption spectra of N3, Y6, BTP-eC9 and L8-BO.

4. PL measurements

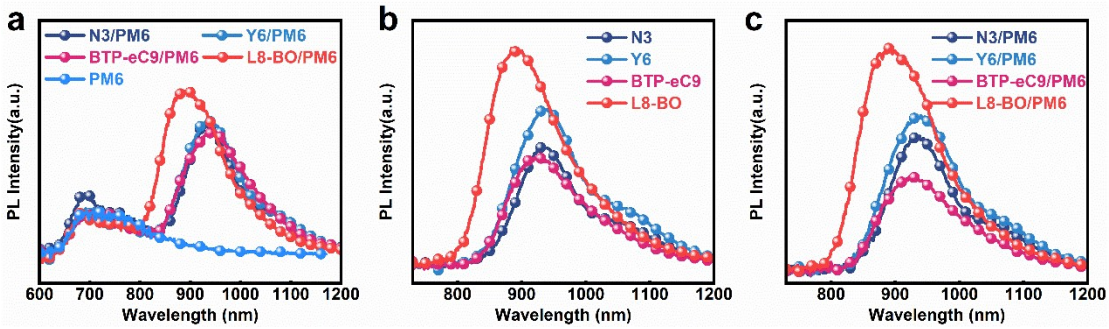

Figure S2. The PL spectra of **(a)** PM6 with and without NFAs, **(b)** different NFAs, **(c)** different NFAs with and without PM6.

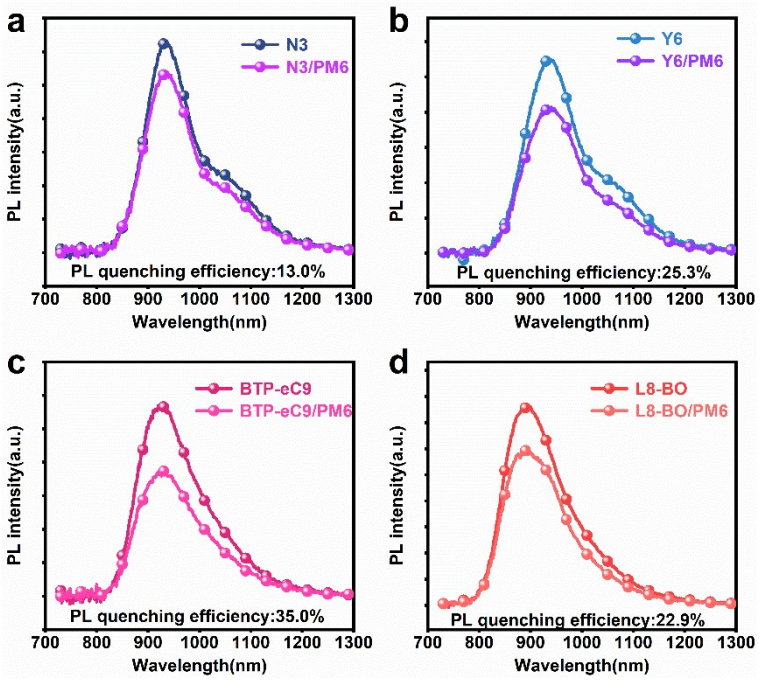

Figure S3. The PL spectra of **(a)** N3 with and without PM6, **(b)** Y6 with and without PM6, **(c)** BTP-eC9 with and without PM6, **(d)** L8-BO with and without PM6.

5. Atomic Force Microscopy (AFM) Measurement

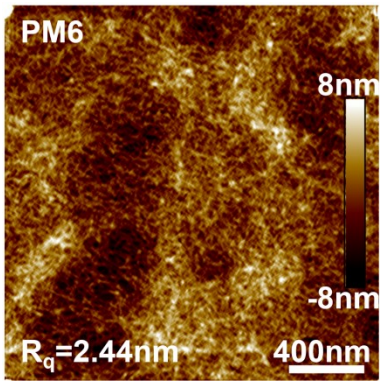

Figure S4. The AFM image of PM6.

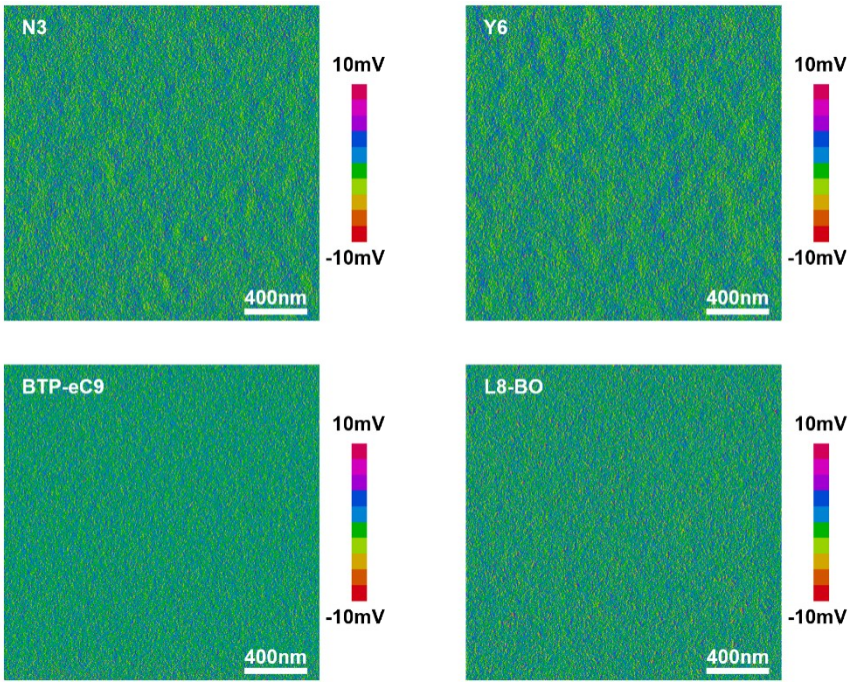

Figure S5. Peak force error topography of **(a)** the N3 film, **(b)** the Y6 film, **(c)** the BTP-eC9 film and **(d)** the L8-BO film.

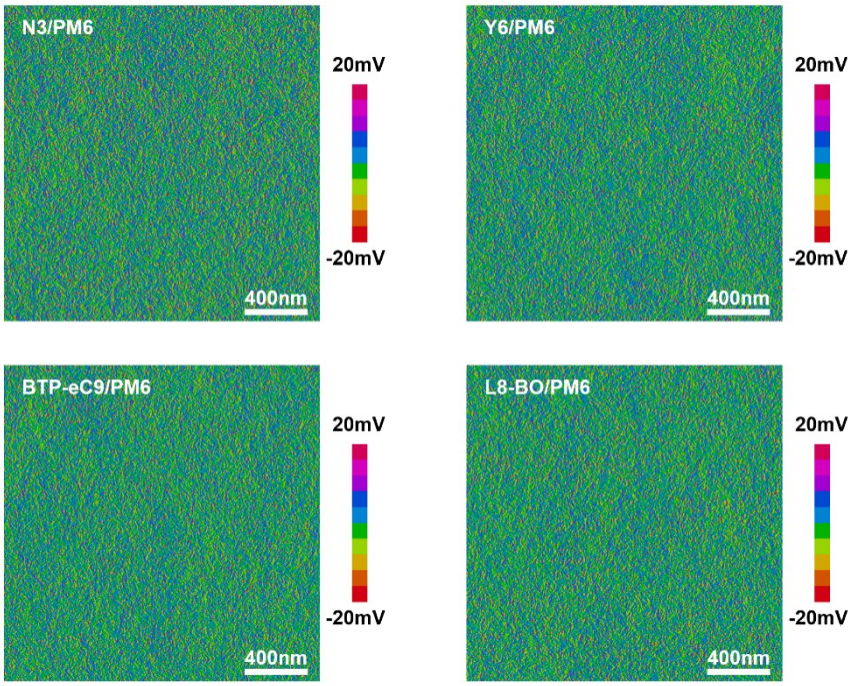

Figure S6. Peak force error topography of **(a)** the N3/PM6 film, **(b)** the Y6/PM6 film, **(c)** the BTP-eC9/PM6 film and **(d)** the L8-BO/PM6 film.

6. GIWAXS measurements

Grazing-incidence wide-angle X-ray scattering (GIWAXS) was carried out to investigate the molecular packing and molecular orientation in the thin films. The π–π stacking distance (d-spacing) and crystalline coherence length (CCL) were calculated quantitatively using the equations d-spacing = $2\pi/q$ and CCL = $2\pi K/\Delta q$, where q, Δq and the K constant represent the peak positions, full width at half maximum. [1,2]

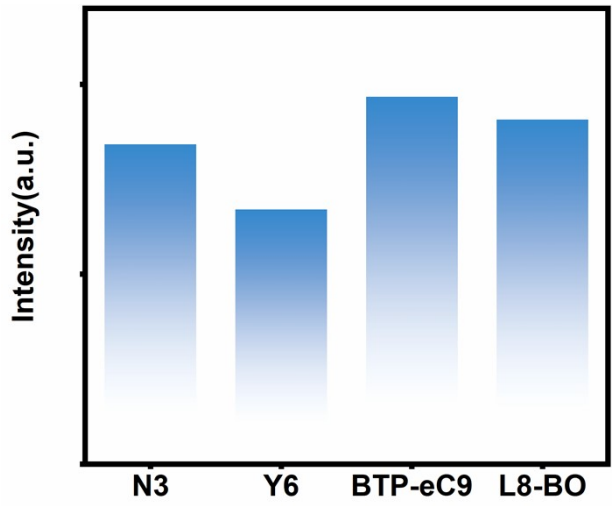

Figure S7. The (010) peak intensity obtained from GIWAXS varies with different NFAs.

Table S1. Out-of-plane parameters; peak location, d-spacing, FWHM, and crystal coherence length (CCL) extracted from the 2D GIWAXS of different NFAs films.

Condition	Peak	Peak location ($Å^{-1}$)	d-space (Å)	FWHM ($Å^{-1}$)	CCL (Å)
N3	(010)	1.73	3.63	0.20	28.27
Y6	(010)	1.71	3.67	0.19	29.76
BTP-eC9	(010)	1.71	3.67	0.28	20.20
L8-BO	(010)	1.70	3.69	0.25	22.44

7. J-V measurements

Table S2. The photovoltaic performance of the optimized inverted bilayer OSCs based on PM6/Y6 changed with the concentration of Y6 under simulated AM1.5G illumination (100 mW cm^{-2}). Values are averaged by ten devices.

Materials	V_{OC} **[V]**	J_{SC} **[mAcm^{-2}]**	***FF*** **[%]**	***PCE*** **[%]**
Y6(16mg/ml)/PM6	890 (888±1)	5.72 (5.42±0.04)	70.93 (70.37±0.85)	3.61 (3.39±0.02)
Y6(14mg/ml)/PM6	885 (883±2)	6.92 (6.44±0.52)	70.01 (69.85±0.51)	4.29 (3.97±0.33)
Y6(12mg/ml)/PM6	892 (887±2)	6.04 (5.75±0.04)	69.53 (69.68±0.29)	3.75 (3.56±0.02)
Y6(10mg/ml)/PM6	888 (886±1)	5.97 (5.69±0.07)	69.36 (68.62±0.52)	3.68 (3.46±0.04)

Table S3. The photovoltaic performance of the optimized inverted bilayer OSCs based on PM6/Y6 changed with the concentration of PM6 under simulated AM1.5G illumination (100 mW cm^{-2}). Values are averaged by ten devices.

Materials	V_{OC} **[V]**	J_{SC} **[mA cm^{-2}]**	***FF*** **[%]**	***PCE*** **[%]**
Y6/PM6(8mg/ml)	881 (880±4)	3.67 (3.52±0.02)	68.88 (68.40±0.85)	2.23 (2.12±0.01)
Y6/PM6(6mg/ml)	893 (892±1)	5.36 (5.12±0.03)	68.64 (68.17±0.63)	3.28 (3.11±0.01)
Y6/PM6(4mg/ml)	885 (883±2)	6.92 (6.44±0.52)	70.01 (69.85±0.51)	4.29 (3.97±0.33)
Y6/PM6(2mg/ml)	873 (879±4)	4.67 (4.35±0.05)	67.53 (67.48±0.19)	2.75 (2.58±0.02)

Table S4. Thickness of PM6 films changed with concentration.

Films	Y6 concentration (mg/mL)	Thickness (nm)
PM6	2 mg/ml	12.3±0.5
	3 mg/ml	34.1±0.2
	4 mg/ml	49.0±0.4
	5 mg/ml	77.3±2.0
	6 mg/ml	96.3±1.4

Table S5. Thickness of Y6 films changed with concentration.

Films	Y6 concentration (mg/mL)	Thickness (nm)
Y6/PM6	10 mg/ml	39.3±3.5
	12 mg/ml	54.0±4.6
	14 mg/ml	82.7±9.1
	16 mg/ml	128±9.5

Table S6. The photovoltaic performance of the optimized inverted bilayer OSCs based on Y6/PM6 changed with solvent additives under simulated AM1.5G illumination (100 mW cm^{-2}). Values are averaged by ten devices.

Materials	V_{OC} **[V]**	J_{SC} **[mAcm^{-2}]**	***FF*** **[%]**	***PCE*** **[%]**
Y6/PM6	885 (883±2)	6.92 (6.44±0.52)	70.01 (69.85±0.51)	4.29 (3.97±0.33)
Y6/PM6(CN)	889 (887±4)	5.51 (5.36±0.01)	70.65 (70.51±0.05)	3.46 (3.36±0.01)
Y6/PM6(BN)	891 (889±3)	5.71 (5.47±0.02)	71.02 (70.52±0.09)	3.61 (3.43±0.01)
Y6/PM6(FN)	886 (888±1)	5.70 (5.46±0.03)	70.40 (70.15±0.19)	3.56 (3.40±0.01)

Table S7. The photovoltaic performance of the optimized inverted bilayer OSCs based on Y6/PM6 changed with solid additives under simulated AM1.5G illumination (100 mW cm^{-2}). Values are averaged by ten devices.

Materials	V_{OC} **[V]**	J_{SC} **[mAcm^{-2}]**	***FF*** **[%]**	***PCE*** **[%]**
Y6/PM6	885 (883±2)	6.92 (6.44±0.52)	70.01 (69.85±0.51)	4.29 (3.97±0.33)
Y6/PM6(TCB)	883 (884±1)	5.63 (5.45±0.03)	69.31 (68.72±0.56)	3.44 (3.30±0.01)
Y6/PM6(TBB)	885 (884±7)	5.73 (5.45±0.04)	69.11 (69.04±0.34)	3.51 (3.32±0.01)
Y6/PM6(TIB)	880 (879±1)	5.28 (5.05±0.02)	67.95 (67.40±0.33)	3.16 (2.99±0.01)

8. EQE measurements

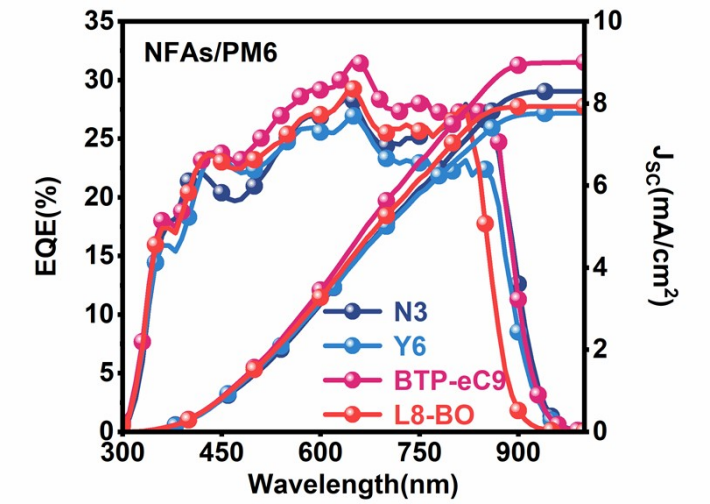

Figure S8. EQE spectra of invert bilayer OSCs based on different NFAs.

9. DLTS measurements

In this experiment, a method of transient photocurrent was used to the DLTS measurement. [3, 4] In there, when a bias of 0V was applied the traps in space charge region were populated, and after a reverse bias of -2.5V used the trap filled can emit the captured charge carriers for heating up to a new bias condition. The carrier emission process is observed as a current transient in the device current signal. By following equation according to experimental data the trapped defect state volume density N_t can be given:

$$j_{te}(t) = \frac{1}{\tau_{te}} \cdot q \cdot d \cdot N_t \cdot exp\left(-\frac{t}{\tau_{te}}\right) \quad (4)$$

Here, j_{te} is trap emission current, τ_{te} is catch-trap emission time constant, q is a single charge amount, d is the thickness of the device [5, 6].

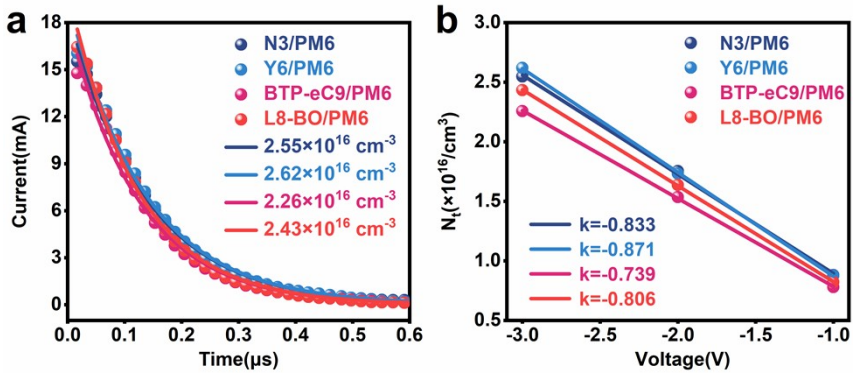

Figure S9. **(a)** Deep-level transient spectroscopy (DLTS) of inverted devices with different NFAs. **(b)** The change of DLTS with the NFAs.

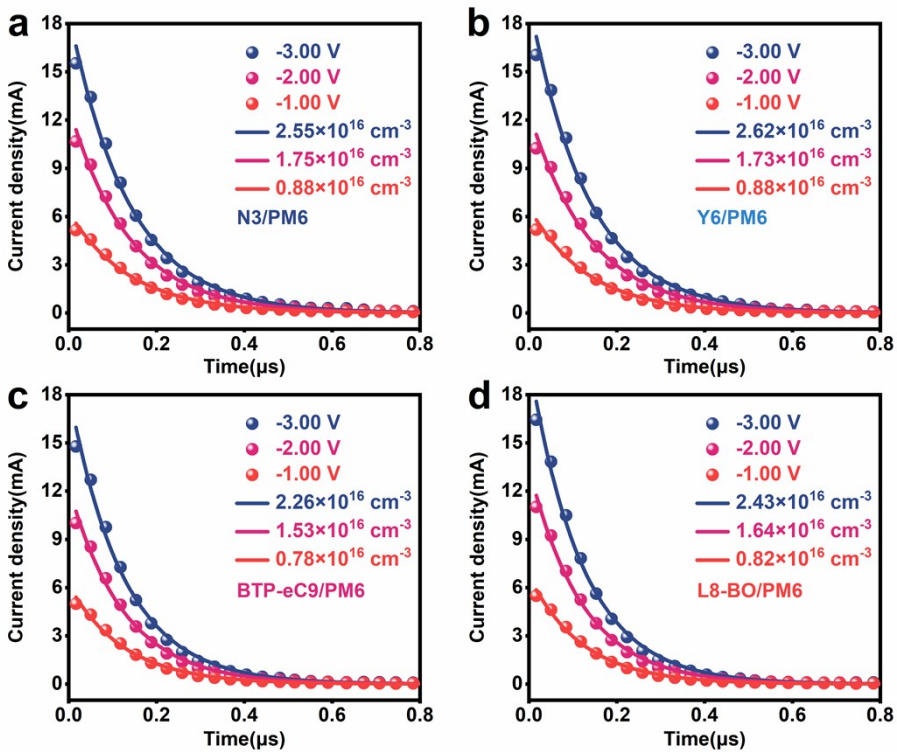

Figure S10. **(a)** Deep-level transient spectroscopy (DLTS) of inverted devices with different NFAs. **(b)** The change of DLTS with the NFAs.

10. Stability measurements

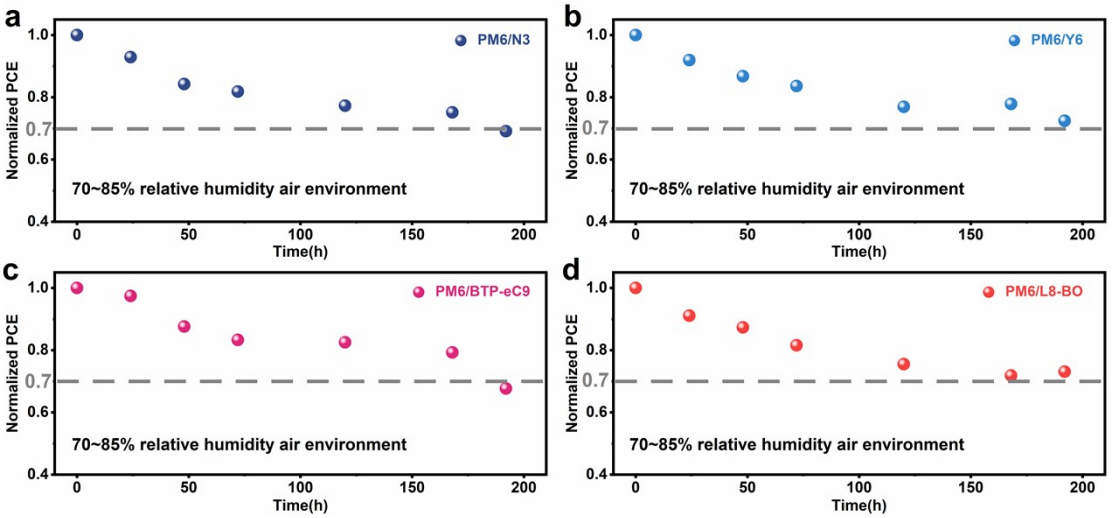

Figure S11. Stability measurements of inverted OSCs based on bulk heterojunctions (BHJ). Degeneration of PCE based on **(a)** PM6:N3, **(b)** PM6:Y6, **(c)** PM6:BTP-eC9 and **(d)** PM6:L8-BO.

11. References

[1] Y. Qin, Y. Xu, Z. Peng, J. Hou, H. Ade. Low Temperature Aggregation Transitions in N3 and Y6 Acceptors Enable Double-Annealing Method That Yields Hierarchical Morphology and Superior Efficiency in Nonfullerene Organic Solar Cells. *Adv. Funct. Mater.* **2020,** *30,* 2005011.

[2] R. Sun, Q. Wu, J. Guo, T. Wang, Y. Wu, B. Qiu, Z. Luo, W. Yang, Z. Hu, J. Guo, M Shi, C. Yang, F. Huang, Y. Li, J. Min . A Layer-by-Layer Architecture for Printable Organic Solar Cells Overcoming the Scaling Lag of Module Efficiency. *Joule.* **2020,** *4,* 407-419.

[3] D. Bozyigit, M. Jakob, O. Yarema, V. Wood. Deep Level Transient Spectroscopy (DLTS) on Colloidal-Synthesized Nanocrystal Solids. *ACS Appl. Mater. Interfaces.* **2013,** *5,* 2915−2919.

[4] R. Li, B. Li, X. Fang, D. Wang, Y. Shi, X. Liu, R. Chen, Z. Wei. Self-Structural Healing of Encapsulated Perovskite Microcrystals for Improved Optical and Thermal Stability. *Adv. Mater.* **2021,** *33*, 2100466.

[5] Z. Zhao, S. Chung, L. Tan, J. Zhao, Y. Liu, X. Li, L. Bai, H. Lee, M. Jeong, K. Cho, Z. Kan. Molecular Order Manipulation with Dual Additives Suppressing Trap Density in Non-Fullerene Acceptors Enables Efficient Bilayer Organic Solar Cells. *Energy Environ. Sci.,* **2025,** *18,* 2791-2803.

[6] Z. Zhao, S. Chung, L. Bai, J. Zhang, Y. Liu, L. Tan, A. Azeez, Y. Huang, E. Ok, K. Cho, Z. Kan, S. Karuthedath. Solubility-Driven Acceptor Fibrilization Enables Bilayer Organic Solar Cells with Efficiency Approaching 20%. *Adv. Funct. Mater.,* **2025,** *35,* 2506593.